ORIENTAL JOURNAL OF CHEMISTRY
An International Open Access, Peer Reviewed Research Journal
www.orientjchem.org
ISSN: 0970-020 X
CODEN: OJCHEG
2024, Vol. 40, No.(6):
Pg. 1715-1722

Synthesis, Biological and *In silico* Studies of (1H-Indol-3-ylmethylene)-naphthalen-1-ylamine and its Os(VIII), Pd (II), Ni(II), Cr (III) and Fe(III) Complexes

UCHECHUKWU SUSAN ORUMA[1]*, PIUS OZIRI UKOHA[1], NKECHINYERE NWANNEKA UKWUEZE[1], LILIAN CHINENYE EKOWO[2], ADAUDE EUPHEMIA AMALUNWEZE[3], SUNDAY NWANKWO OKAFOR[4] and SOLOMON EJIKE OKEREKE[5]

[1]Coordination Chemistry and Inorganic Pharmaceuticals Unit, Department of Pure and Industrial Chemistry, University of Nigeria, Nsukka, 410001, Nigeria.
[2]Department of Pure and Industrial Chemistry, University of Nigeria, Nsukka, 410001, Nigeria.
[3]Department of Science Laboratory Technology, Federal Polytechnic, Oko.
[4]Department of Pharmaceutical and Medicinal Chemistry, University of Nigeria, Nsukka 410001, Nigeria.
[5]Department of Industrial Chemistry, Abia State University, Uturu, Abia State.
*Corresponding author E-mail: susan.oruma@unn.edu.ng

http://dx.doi.org/10.13005/ojc/400624

(Received: June 26, 2024; Accepted: December 2, 2024)

ABSTRACT

(1H-Indol-3-ylmethylene)-naphthalen-1-ylamine, INDNA was synthesized by the condensation of 1-naphthylamine with indole-3-carboxaldehyde. Additionally, the complexes of Os(VIII), Pd (II), Ni(II), Cr(III) and Fe(III) were synthesized. ESI-MS spectroscopic techniques, ^{1}H and ^{13}C NMR, UV-VIS, IR and elemental analysis were used to characterize the ligand and metal complexes. According to spectral data, INDNA binds as a bidentate ligand to the metal ions via the nitrogens in the imine and indole chains. The ligand to metal stoichiometry of the compounds is 2:1. The metal complexes exhibit tetrahedral geometry. The ligand and complexes were tested for their *in vitro* antibacterial activity against a range of microorganisms namely: *Salmonella* sp., *Staphylococcus* sp. (vancomycin resistant), *Candida albicans*, *Klebisella* sp. (pneumonia), *Sewage-producing* sp., clinical sp., and typed sp. using agar well diffusion method. Compared to the ligand, the complexes were found to be more active against the tested bacteria. The antifungal activity of INDNA was enhanced on complexing with Pd(II) ion. The drug likenesses were also determined using molecular docking studies.

Keywords: Schiff base ligand, Os(VIII), Pd(II), Ni(II), Cr(III) and Fe(III) complexes, Antimicrobial activities, Docking.

INTRODUCTION

Metal complexes of Schiff base ligands containing donor atoms of nitrogen and oxygen are known to exhibit interesting physicochemical properties as well as physiological activities[1-8].

They are of great importance in bioinorganic chemistry because they provide synthetic models for metal-containing sites in metallo-proteins and metallo-enzymes[9,10]. They have been widely studied not only because of their biological importance, but also because many of them show unusual magnetic properties, novel structural features and catalytic activities[11]. Metal complexes of indole have gained much attention due to their biological and pharmacological properties. These complexes have been shown to be effective as antimicrobial, anticancer, antiviral, antiplatelet aggregation, anticonvulsant and antihypertensive agents[12-15]. They have also been applied in bio-imaging because they are bio-compatible and have excellent sensing application in aqueous media[16]. A number of Schiff bases generated from indole along with associated metal complexes have been synthesized, characterized and their biological activities studied[17-20]. The different types of bonding of the indole ring with transition metals have been reported[21-22]. Also, bidentate N,N-donor ligands derived from indole and their metal complexes have been reported[23-25]. According to these investigations, the metal complexes exhibit more powerful actions than the ligands. This is due to its chelating properties and enhanced lipophilicity of the resulting complexes with transition metals. However, some of these complexes may have side effects like gastrointestinal disorder, allergic reactions or organ-specific toxicities[26].

(1H-Indol-3-ylmethylene)-naphthalen-1-ylamineis is a Schiff base derived from 1-naphthylamine and indole-3-carboxaldehyde in methanol. Research has demonstrated that the addition of the lipophilic naphthalene ring increases the ability of Schiff bases to pass across different types of bio-membranes[27–30]. The easily accessible literature search reveals that the Os(VIII), Pd(II), Ni(II), Cr(III) and Fe(III) complexes of (1H-Indol-3-ylmethylene)-naphthalen-1-ylamine, as well as their synthesis and characterization, have not been studied. Their use in biological research has not been documented. In view of the need for more potent antimicrobials with less side effect, we synthesized, characterized and determined the antimicrobial property of (1H-Indol-3-ylmethylene)-naphthalen-1-ylamine and its Os(VIII), Pd (II), Ni(II), Cr(III) and Fe(III) complexes. The ligand's drug likeness was also determined using molecular docking studies.

EXPERIMENTAL

Unless otherwise indicated, every reagent and solvent used was of analytical grade and was used exactly as given. The compounds melting points(uncorrected) were obtained using Fisher-Johns melting point apparatus. Using a CE9050 Cecil UV-Vis spectrophotometer, electronic spectra were captured. Nujol mull was used to record the IR spectra on a Mattson Genesis II Fourier Transform IR spectrophotometer, model number 960M000, in the 4000-400 cm^{-1} range. The ^{1}H and ^{13}C NMR spectra were recorded in $CDCl_3$+CD_3OD on a Varian Mercury-200B "oauife" NMR spectrophotometer.. Job's continuous variation method was used to determine the combining ratio of metal to ligand in the complexes[31].

Synthesis of (1H-Indol-3-ylmethylene)-naphthalen-1-ylamine, INDNA

To a solution of indole-3-carboxaldehyde (4839mg, 33mmol) in methanol (42.5mL) was added 1-naphthylamine (4773mg, 33mmol) with stirring. After adding a few 4A0 molecular sieves, the mixture reacted for five days at room temperature. It was observed that some little quantity of the solvent evaporated. The sieves were later removed and the brown crystals formed were collected and recrystallized from methanol to give a light brown granular compound. This was dried and stored in a desiccator. Yield: 79.89%, colour: Light brown, soluble in DMSO, DMF, Dicloromethane. ^{1}H NMR: Chemical shift (δ) in ppm: 7.18-8.29 (multiplets, aromatic H), 8.55 (d, 1H, indole H), 8.83 (s, 1H, azomethine), 9.95 (s,1H, Indole N-H). ^{13}C NMR: Chemical shift (δ) in ppm: 184.96(azomethine Carbon), 138.45(aromatic carbon on naphthalene ring), 137.06 (indole carbon), 112.17–133.65 (aromatic carbon). FTIR (KBr, cm^{-1}): 3350(indole-N-H), 3100 (Aromatic–C-H), 1600 (Aromatic C=C), 1580 (azomethine C = N), 1450 (naphthalene-C-H), 720 (N-H wag). UV/Visible(λnm) (DMSO): 284. Mass: (m/z) 271.1, (m+1) = 272.2(supplementary material Figure 1-4).

Synthesis of metal complexes of (1H-Indol-3-ylmethylene)-naphthalen-1-ylamine

(1H-Indol-3-ylmethylene)-naphthalen-1-ylamine (360mg, 1.33mmol) was dissolved in dichloromethane (10 mL) and added to methanol (10 mL) solution of the metal salts (0.67mmol)

respectively. The metal salts used are: chromium(III) nitrate nonahydrate, palladium(II) chloride, Osmium tetraoxide, iron(III) chloride, nickel(II)chloride. For an hour, the mixture was stirred. The precipitates obtained were filtered and recrystallized from diethyether. This was allowed to dry naturally and kept over anhydrous $CaCl_2$ in a desiccator.

Cr(III) Complex of INDNA

Yield: 57%, colour: Dark green. ^{1}H NMR: Chemical shift(δ) in ppm: 721-7.84 (multiplets, aromatic H), 8.30 (d, 1H, indole H), 9.35 (s, 1H, azomethine), 10.02 (s,1H, Indole N-H). ^{13}C NMR: Chemical shift (δ) in ppm: 185.24 (azomethine Carbon), 136.76 (aromatic carbon on naphthalene ring), 135.76 (indole carbon), 111.68–124.30 (aromatic carbon). FTIR (KBr, cm^{-1}): 3100 (indole-N-H), 3000 (Aromatic–C-H), 1600 (Aromatic C = C), 1595 (azomethine C = N), 1400 (naphthalene-C-H), 1300 and 1310 (covalent NO_3-), 800 (N-H wag), 600 (M-O), 420(M-N). UV/Visible(λnm) (DMSO): 198, 299. (supplementary material Figure 5-7).

Fe(III) Complex of INDNA

Yield: 64%, colour: Black. ^{1}H NMR: Chemical shift (δ) in ppm: 7.19-8.25 (multiplets, aromatic H), 8.36 (d, 1H, indole H), 8.47 (s, 1H, azomethine), 9.92 (s,1H, Indole N-H). ^{13}C NMR: Chemical shift(δ) in ppm: 184.57 (azomethine Carbon), 138.17(aromatic carbon on naphthalene ring), 136.52 (indole carbon), 111.99–123.57 (aromatic carbon). FTIR (KBr, cm^{-1}): 3300 (indole-N-H), 3100 (Aromatic–C-H), 1600 (Aromatic C = C), 1560 (azomethine C = N), 1400(naphthalene-C-H), 950(N-H wag), 450(M-N). UV/Visible(λnm) (DMSO): 287, 475. (supplementary material Figure 14-16).

Ni(II) Complex of INDNA

Yield: 56%, colour: Milky. ^{1}H NMR: Chemical shift(δ) in ppm: 7.12-8.25 (multiplets, aromatic H), 8.49 (d, 1H, indole H), 8.78 (s, 1H, azomethine), 10.00 (s,1H, Indole N-H). ^{13}C NMR: Chemical shift(δ) in ppm: 184.17(azomethine Carbon), 154.91(aromatic carbon on naphthalene ring), 149.35 (indole carbon), 111.46–133.77 (aromatic carbon). FTIR (KBr, cm^{-1}): 3200 (indole-N-H), 3100 (Aromatic–C-H), 1600(Aromatic C = C), 1580(azomethine >C = N), 1430 (naphthalene-C-H), 800(N-H wag), 450 (M-N). UV/Visible(λnm) (DMSO): 280, 305. (supplementary material Figure 17-19).

Pd(II) Complex of INDNA

Yield: 87%, colour: Yellow. ^{1}H NMR: Chemical shift(δ) in ppm: 7.34-7.86 (multiplets, aromatic H), 8.33 (d, 1H, indole H), 9.06 (s, 1H, azomethine), 10.06 (s,1H, Indole N-H). ^{13}C NMR: Chemical shift(δ) in ppm: 185.23 (azomethine Carbon), 136.68 (aromatic carbon on naphthalene ring), 135.44 (indole carbon), 111.57–124.42 (aromatic carbon). FTIR (KBr, cm^{-1}): 3300 (indole-N-H), 3150 (Aromatic–C-H), 1600 (Aromatic C = C), 1595 (azomethine C = N), 1410 (naphthalene-C-H), 800 (N-H wag), 450 (M-N). UV/Visible (λnm) (DMSO): 218, 291, 375. (supplementary material Figure 8-10).

Os(VIII) Complex of INDNA

Yield: 46%, colour: Light pink. ^{1}H NMR: Chemical shift(δ) in ppm: 7.27-7.85 (multiplets, aromatic H), 8.38 (d, 1H, indole H), 9.06 (s, 1H, azomethine), 10.06 (s,1H, Indole N-H). ^{13}C NMR: Chemical shift(δ) in ppm: 185.26 (azomethine Carbon), 136.72 (aromatic carbon on naphthalene ring), 135.51 (indole carbon), 111.61–124.43 (aromatic carbon). FTIR (KBr, cm^{-1}): 3300 (indole-N-H), 3150 (Aromatic–C-H), 1600 (Aromatic C = C), 1550 (azomethine C = N), 1400(naphthalene-C-H), 800 (N-H wag), 610 (M-O), 450(M-N). UV/Visible (λnm) (DMSO): 199, 250, 295. (supplementary material Figure 11-13).

Stoichiometry of the complexes

A solution of INDNA (10^{-3} M), and the metal salts were prepared respectively. The ligand was combined with varying quantities of the metal salts so that the mixture's total volume at each run was equal to 10 mL. Absolute ethanol (5 mL) was added into each mixture making a total of 15 mL each. These mixtures were corked, shaken and kept to react for 30 minute. The absorbance of each of the mixtures was determined at a suitable wavelength. Next, a plot was made showing the absorbance vs the volume fraction, which represents the reactant mole ratio. The mole ratio was determined by extrapolation from the curve.

Antimicrobial activity

The agar well diffusion method in dimethyl sulphoxide (DMSO) was used to investigate the antibacterial properties of the produced compounds.[32] *Pseudomonas* sp. (clinical), *Pseudomonas* sp. (sewage), *Pseudomonas* sp. (typed), *Klebisella* sp. (4A), *Klebisella* sp. (4B), *Klebisella* sp. (pneumonia), *Salmonella* sp., *Staphylococcus* sp.(vancomycin

resistant) and *Candida albicans* were used in the antimicrobial studies. These microorganisms have been known to be multi-drug resistant[33]. The turbidity of each test organism colony was adjusted to satisfy the 0.5 MacFarland threshold while it was suspended in sterile normal saline. Colony forming units (cfu) from each bacterial and fungal suspension were applied to the surface of sterile Mueller Hinton agar plates. After letting the plate surfaces dry, the agar plates were drilled with wells using a sterile cork borer with a 6 mm diameter. To each well, 100μg/mL of the synthesized compounds was introduced. Other wells were supplemented with antibacterial drugs namely ciprofloxacin, gentamicin and antifungal drug nystatin, which serve as positive control while the negative control was the well containing DMSO. For a whole day, the plates were incubated at 37°C. Zones of inhibition (ZID) diameter were expressed in millimeters.

Molecular Docking

The mode of interactions and possible mechanism of action of the synthesized complexes with the relevant microbial drug targets were further studied using molecular docking simulation. The crystal structure of PqsR co-inducer binding domain of, an important drug target in *Pseudomonas aeruginosa*, was retrieved from Protein Databank (https://www.rcsb.org/structure/4JVI). The protein was prepared using Discovery Studio v24 20, whereby multiple chains, unwanted molecules and water of crystallization were removed[34]. Both the synthesized compound and the prepared protein were energy minimized. The compound and the reference drug, ciprofloxacin, were docked into the active binding sites of the protein and the docking scores calculated.

RESULTS AND DISCUSSION

The reaction of indole-3-carboxaldehyde with 1-napthylamine yielded 1-napthylimino-indole-3-carboxaldehyde, INDNA as shown in Scheme 1.

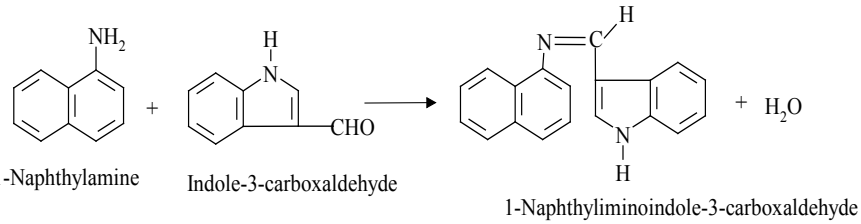

Scheme 1: Synthesis of INDNA

The synthesized metal complexes, $[Cr(NO_3)_2(INDNA)_2]^+$, $[Pd(INDNA)_2]Cl_2$ and $[Os(INDNA)_2O_2]^{4+}$ were all found to exist in 1:2 metal to ligand stoichiometry. Table 1 lists the ligand and complexes' physicochemical characteristics. The Os (VIII) complex was the only one of the produced compounds that was crystalline.

Table 1: Physical and Elemental data of INDNA and its Os(VIII), Pd(II), Ni(II), Cr(III) and Fe(III) complexes

Compound/Mol. formula	Colour	Yield(%)	m.p. (°C)	Molar mass (g/mol)	Elemental analysis % calc. and found					
					C		H		N	
					Calc.	Found	Calc.	Found	Calc.	Found
$C_{19}H_{14}N_2$	Light-brown	79.89	162	270	84.44	84.23	5.19	5.10	10.37	9.8
$C_{38}H_{28}N_7O_9Cr$	Dark-green	57	132	777	58.69	59.8	3.60	4.0	12.61	12.30
$C_{38}H_{28}N_4Cl_2Pd$	Yellow	87	205	717	63.60	63.40	3.91	4.4	7.81	7.9
$C_{38}H_{28}N_4O_6Os$	Light-pink	46	183	830	54.94	54.40	3.86	3.9	6.75	6.9
$C_{38}H_{28}N_4Cl_3Fe$	Black	64	> 300	702.50	64.91	64.6	3.98	4.6	7.97	7.8
$C_{38}H_{28}N_4Cl_2Ni$	milky	56	> 300	669.69	68.06	67.80	4.17	4.8	8.36	8.00

Electronic spectra

The INDNA and complexes (10^{-4} $moldm^{-3}$) UV/Vis absorption spectra were measured at room temperature in DMSO. The compounds' electronic absorption spectra display bands ranging from 198 to 305 nm, which correspond to the π–π* and n–π* transitions of the azomethine group and conjugated phenyl ring, respectively. In the Pd(II) complex, the band at 375 nm was assigned to $^1A_{1g}$-$^1E_{2g}$. The electronic spectra of Pd(II) complexes in square planar environment usually show two spin allowedd-d transitions : $^1A_{1g}$-$^1B_{1g}(\upsilon_1)$ and $^1A_{1g}$-$^1E_{2g}(\upsilon_2)$ observed between 21740-18250

and 26320-22200 cm^{-1} respectively[35-36]. The spectrum of $[Os(INDNA)_2O_2]^{4+}$ reveals three bands all in the ultraviolet region ranging from strong to moderate intensities. No band was observed in the visible region. This is in accordance with reports on Os(VIII) complexes[37], since it is a d^0 complex. The light pink colour of this complex gives an insight that its transition is largely due to charge transfer. Similar observation has been made with other d^0 complexes[38].

Infrared Spectra

The broad bands seen in INDNA and complexes between 3350–3100 cm^{-1} and 800-750 cm^{-1}, respectively, were attributed to indole υ (N–H) stretching and rocking vibrations[39-40]. The shift of these bands to lower wavenumber in the complexes suggests participation of the indole nitrogen in bonding to the metal ions. At 1580 cm^{-1}, a medium band containing the C = N stretching vibration was detected in the ligand. This band shifted to higher and lower wavenumbers within the complexes. This suggests that the imine nitrogen caused ligation to occur. Literature has also made similar observations[41]. The Cr(III) complex showed a new band at 1300 and 1310 cm^{-1}, which may be due to covalently bonded nitrate. Previous studies have demonstrated that two prominent bands in nitrate complexes, occurring in 1550–1535 cm^{-1} and 1315–13300 cm^{-1}, respectively, are attributed to the υ_4 and υ_1 modes of vibration of covalently bound nitrate groups[42]. This implies that the coordination sphere contains the nitrate groups. In $[Os(NICA)_2O_2]^{4+}$, existence of band at 610 cm^{-1} assignable to M-O confirms oordination of Os (VIII) to oxygen atom. All of the complexes exhibit faint bands in the 450–420 cm^{-1} area that are attributed to υ (M–N), which supports ligation through the nitrogen atom[43].

^{1}H and ^{13}C NMR

At ambient temperature, the ^{1}H and ^{13}C NMR spectra of INDNA and its complexes were recorded in $CDCl_3$+CD_3OD using tetramethylsilane (TMS) as the internal reference compound. The difference in chemical shift of the azomethine proton and indole N-H proton of the ligand and complexes served as an evidence of coordination through their nitrogen atoms. The N = C - H signal for the compounds were observed between 9.35- 8.47 ppm. Similar report has been made in earlier published works[43]. The indole N-H signal was observed between 10.06-9.92 ppm for the compounds. The peaks assigned to aromatic protons were observed as multiplets in the range 7.12-8.29 ppm in all the compounds.

Table 2: ^{13}C NMR assignment for INDNA and its metal complexes

compound	C11(ppm)	C10(ppm)	C13(ppm)	Aromatic carbon	Structure of INDNA showing carbon numbering
NICA	184.96	138.45	137.06	112.17–133.65	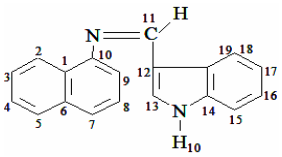
Cr(III) complex	185.24	136.76	135.76	111.68–124.30	
Pd(II) complex	185.23	136.68	135.44	111.57–124.42	
Os(VIII) complex	185.26	136.72	135.51	111.61–124.43	
Fe(III) complex	184.57	138.17	136.52	111.99–123.57	
Ni(II) complex	184.17	154.91	149.35	111.46–133.77	

The ^{13}C NMR of INDNA (Table 2) revealed a downfield signal at 184.96 ppm and 138.45 ppm assignable to C11 and C10. In the complexes, these signal differ by about 1.70 ppm which suggest coordination through the imine nitrogen and indole nitrogen. Other signals observed were attributed to aromatic carbons.

The structure in Fig. 1 has been suggested for the complexes based on the results of the spectral data.

Antimicrobial activity

Table 3 shows the inhibitory zone diameter (IZD) of the drugs against multidrug resistant bacteria. The Pd(II) complex gave the highest broad spectrum antimicrobial activities relative to all the compounds. It showed moderate activities against all the tested microorganisms except *Salmonella* species. It also showed more activity against *Candida albicans* relative to INDNA. This reveals that the antimicrobial activity of INDNA can be enhanced by complexing with Pd (II) ion. Its Cr (III) complex, was active against *Pseudomonas* species(clinical), *Klebisella* species(4A), and Vancomycin resistant *Staphylococcus aureus* species.

***In silico* Studies**

The binding free energy of the ligand with the drug target is shown in Table 4.

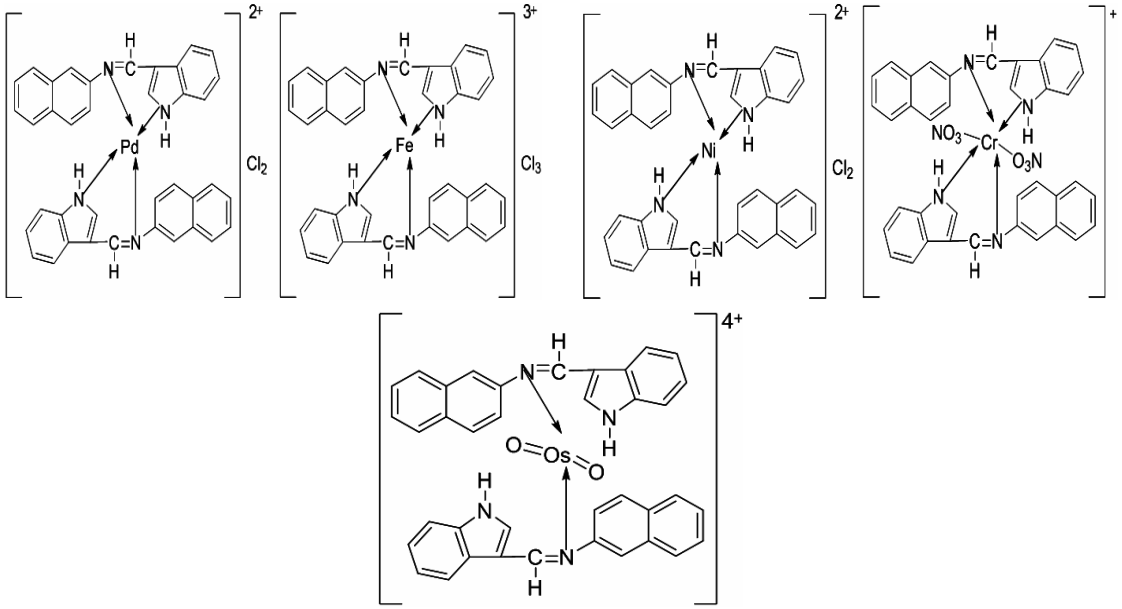

Fig. 1. Proposed structure of the complexes

Table 3: Compounds' Inhibition Zone Diameter (IZD in mm)

Organism	Controls ciprofloxacin	INDNA (100 μg/mL)	Pd(II) complex (100 μg/mL)	Cr(III) complex (100 μg/mL)	Fe(III) Complex	Ni(II) Complex
P. sp (clinical)	30	9.5	14	9	7	8
P. sp (sewage)	30	9.5	10	-	6.5	7
P.sp (typed)	28	9.0	10	-	6	7.5
K.sp (4A)	25	8.5	10	-	-	-
K. sp (4B)	32	9.0	18	13	-	-
K.sp (pneumonia)	30	-	13	-	-	-
Sal. sp	45 Gentamicin	9	-	-	-	8
Staph.sp	23 Nystatin	8	15	14	5	-
Candida albicans	17	9	13	-	5	7

Table 4: Binding free energy, ΔG (kcal/mol)

Compound	Ciprofloxacin	Natïve ligand	Synthesized Ligand
Docking score	-6.04	-6.75	-5.74

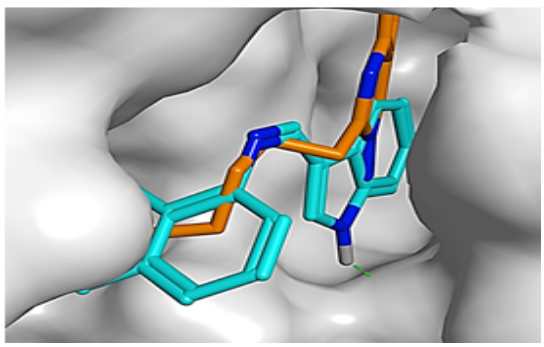

Fig. 2(a). Synthesized ligand in the active binding site of *Pseudomonas aeruginosa* quorum sensing regulaor PqsR (MvfR)(PDB: 4JVI)

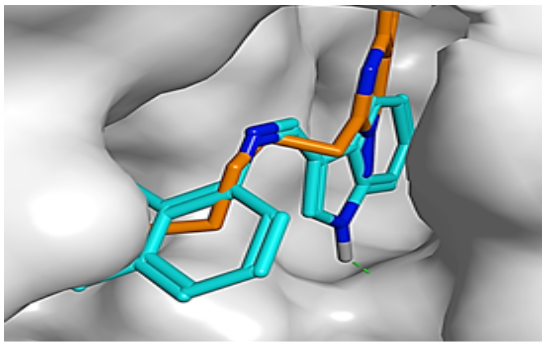

Fig. 2(b). Ligand (cyan) and co-crystallized ligand (orange) in the active binding site of *Pseudomonas aeruginosa* quorum sensing regulaor PqsR (MvfR)

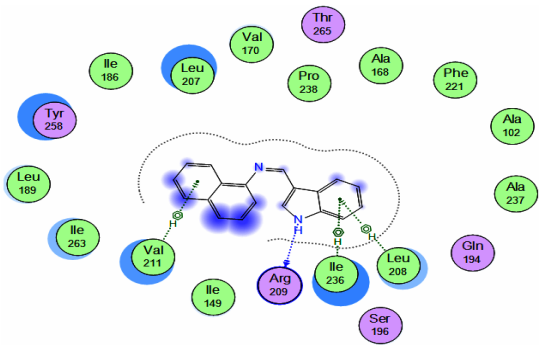

Fig. 3. The two-dimensional depiction of the ligand-receptor amino acid residue binding interactions

Table 5: Receptor-ligand interactions of ligand with Pseudomonas aeruginosa quorum sensing regulaor PqsR (MvfR)

Ligand	Receptor	Interaction	Distance (Å)	E (kcal/mol)
N 6	OARG 209	H-donor	3.06	-2.5
6-ring	CALEU 208	pi-H	4.10	-0.3
6-ring	CG1VAL 211	pi-H	4.25	-0.3
6-ring	CBILE 236	pi-H	4.24	-0.4
6-ring	CD1ILE 236	pi-H	3.83	-0.4

The ligand tightly fit into the binding site of the *Pseudomonas aeruginosa* quorum sensing regulator PqsR (MvfR) as shown in Fig. 2a, occupying the same binding cavity as the co-crystallized ligand (Fig. 2b). This gives credence to the molecular docking validation protocol which resulted in the observed docking score of 5.74 kcal/mol as shown in Table 4. The precise two-dimensional (2D) interactions between the ligand's atoms and the therapeutic target's amino acid residues were displayed in Fig. 3 and Table 5. There were various effective chemical interactions. The N7 atom of the ligand, through H-bonding, interacted with the O atom of ARG209. Also, the pi electrons of the 6-membered ring in the indole moiety formed pi-H bonds with LEU208 and ILE236 while the 6-membered ring in naphthalene group also contributed a pi-bonding interaction with the CG1 of VAL211. The ligand was able to inhibit the *P. aeruginosa* quorum sensing (QS) system, which regulates the expression of hundreds of genes, many of which code for virulence factors.

CONCLUSION

(1H-Indol-3-ylmethylene)-naphthalen-1-ylamine, INDNA derived from 1-naphthylamine and indole-3-carboxaldehyde and its Cr(III), Pd(II) and Os(VIII), Fe(III) and Ni(II) complexes were synthesized.

Based on analytical and spectral data, INDNA coordinates to the metal ions as a monobasic bidentate NN donor via its indole nitrogen and imine nitrogen atoms.

The metal complexes were assigned a tetrahedral shape.

The Pd(II) complex showed the strongest broad spectrum antibacterial activity relative to the synthesized compound.

The molecular docking revealed that the ligand was able to inhibit the *P. aeruginosa* quorum sensing (QS) system.

ACKNOWLEDGEMENT

Prof. K. F. Chah of the University of Nigeria, Nsukka's Department of Veterinary Pathology and Microbiology is appreciated by U. S. Oruma for conducting the antimicrobial test on the synthetic compounds. She also thanks Late Mrs. Chinelo Alioke for her efforts in doing the laboratory work.

Conflict of interest

There are no disclosed conflicts of interest by the authors.

REFERENCES

1. Jain, A.; De, S.; Barman, P., *Resear. on Chemi. Intermdiates.*, **2022**, *48*(5), 2199 – 2251. https://doi.org/10.1007/s11164-022-04708-7.
2. Tajuddin, A. M.; Hadariah, B.; Kassim, K.; Nazihah, W. I. W.(2014)., *ASEAN Journal on Science and Tech.*, **2014**, *31*(1), 15. DOI: 110.29037/ajstd.24.
3. Salehzadeh, S.; Golbedaghi, R.; Rakhtshah, J.; Adams, H., *J. Mol. Struct.*, **2021**, *1245*. 1309882. https://doi.org/10.1016/j.molstruc.2021.130982
4. Oliveira, R. S.; Gaspar, M. H. S.; Pereira, T. R. C.; Fracaro, J. E.; Ballini, M. T., *Coordi-nation Chemistry Reviews.*, **2020**, *368*, 122055. https://doi.org/10.1016/j.ccr.2020.122055.
5. Molnar, M.; Loncaric, M.; Gaso-Sokac, D.; Jokic, S., *Review, Biomolecules, MDPI.*, **2020**, *10*(151), 1-35; https://doi.org/10.3390/biom10010151.
6. Kostic, M. S.; Rodic, M. V.; Vojinovic-Jesic, L. S.; Radanovic, M. M., *J. Serb. Chem. Soc.*, **2023**, *88*(12), 1253–1264.

7. Abd El-Hamid, S. M.; Sadeek, S. A.; El-Farargy, A. F.; Abd El-Lattif, N. S., *Bulletin of the chemical society of Ethiopia.*, **2021**, *35*(2), 315-335. https://doi.org/10.4314/BCSE.V35I2.12.
8. Meeran, I. S.; Raja, T. W.; Dusthakeer, V. A.; Ali, M. M.; Tajudeen, S.S.; Shabeer, T.K., *New Journal of Chemistry.*, **2022**, *46*(10), 4620-4633. https://doi.org/10.1039/DINJ04977A.
9. El-Gammal, O. A.; Mohamed, F. S.; Rezk, G. N.; ElBindary A. A., *J. Mol.Liq.,* **2021**, *326*, 115-223; https://doi.org/10.1016/j.molliq.2020.115223
10. Joseyphus, R. S.; Nair, M. S., *Arabian Journal of Chemistry.*, **2010**, *3*, 195–201.
11. Singh, A. K.; Niharika, K., *Int. J. Applied Eng. and Tech.*, **2023**, *5*(4), 3389–3393.
12. Cheekatla, S. R.; Barik, D.; Anand, G.; Mol, K.M. R.; Porel, M., *Organics.*, **2023**, *4*, 333-363.
13. Devi, J.; Nadav, J.; Kumar, D.; Jindal, D. K.; Basu, B., *Appl. Organomet. Chem.*, **2020**, *34*, e5815.
14. Oberhuber, N.; Ghosh, H.; Nitzsche, B.; Dandawate, P.; Hopfner, M.; Schobert, R.; Bier-sack, B., *Int. J. Mol. Sci.*, **2023**, *24*, 854.
15. Varma, R. R.; Pandya, J. G.; Vaidya, F. U.; Pathah, C.; Bhatt, B. S.; Patel, M. N., *Chem. Biol. Interact.*, **2020**, *330*. https://doi.org/10.1016/J.CBI.2020.109231.
16. Wang, Z.; Zheng, C.; Xu, D.; Liao, G.; Pu, S., *J. Photochem. Photobiol. A Chem.*, **2022**, *424*. https://doi/10.1016/J.JPHOTOCHEM.2021.113634.
17. Rangaswamy, J.; Ankali, K. N.; Naik, N.; Nuthan, B. R.; Satish, S., *Journal of the Iranian Chemical Society.*, **2022**, *19*, 3993-4004. https://doi.org/10.1007/s13738-022-02580-1.
18. EL-Gammal, O. A.; Alshater, H.; El-boraey, H. A., *J. Mol. Struct.*, **2019**, *1195*, 220–230.
19. Sharma, S.; Meena, R.; Singh, R.V.; Fahmi, N., *Main Group Metal Chemistry.*, **2016**, *39*(1-2), 31-40. https://doi.org/10.1515/mgmc-2015-0030.
20. Abdulghani, A. J.; Hussian, R. R., *Open J. of Inorganic Chemistry.*, **2015**, *5*, 83-101.
21. Yamamoto, K.; Kimura, S.; Murahashi, T., *Angew. Chem. Int. Ed.*, **2016**, *55*, 5322–5326.
22. Shimazaki, Y.; Yajima, T.; Yamauchi, O., *J. Inorg. Biochem.*, **2015**, *148*, 108–115.
23. Babijczuk, K.; Warzajtis, B.; Starzyk, J.; Mrowczynska, L.; Jasiewicz, B.; Rychlewska, U., *Molecules.*, **2023**, *28*, 4132.
24. Wittmann, C.; Sivchenko, A. S.; Bacher, F.; Tong, K.K.; Guru, N.; Wilson, T.; Gonzales, J.; Rauch, H.; Kossatz, S.; Reiner, T., *Inorg. Chem.*, **2022**, *61*, 1456–1470.
25. Sahar, Y. J.; Mohammed, H.; Al-Abady, Z. N., *Results Chem.*, **2023**, *5*, 100847.
26. Abdulla Al Awadh, A., *Saudi Pharmaceutical Journal*, **2023**, *31*, 101698, 1-14.
27. Maiti, S. K.; Bora, A.; Barman, P.; Chandra, A. K.; Baidya, B., *Journal of Coordination Chemistry.*, **2020**, *73*(1), 67–86.https://doi.org/10.1080/00958972.2019.1711069.
28. Adhao, S.T.; Wagh, R.R., *Oriental Journal of Chemistry.*, **2023**, *39*(6), 1571-1578.
29. Abdel-Rahman, L. H.; Abu-Dief, A. M.; Newair, E. F.; Hamdan, S. K.. *Journal of Photo-chemistry and Photobiology B, Biology.,* **2016,** *2*, 18 – 31.
30. Faizul A., Satendra S., Lal K.S. and Om p., *J. of Zheijang University.*, **2007**, *8*(6), 446.
31. Jeffery, G. H.; Bassett, J.; Mendham, J.; Denney, R. C.; Vogel's Textbook of Quantitative Chemical Analysis, 5th Ed., Longman Scientific & Technical, New York., **1989**.
32. Collins, C. H.; Lynes, P. M.; Grange, J. M. Microbiological Methods, 1995, 7th Edition Butterwort-Heinemann Ltd, Britian, 175-190.
33. Poole K., *J. of Inorg. Biochem.*, **2004**, *98*(2), 387-392.
34. BIOVIA, Dassault Systemes, Discovery studios, v24.1.0.23298 San Diego: Dassault Sys-temes, **2024**.
35. Yadav, P. N.; Bhattrai, L.; Mehta, P. K., *J. Nepal Chem. Soc.*, **2011**, 28.
36. Ajibade, P. A.; Idemudia, O. G., *Bioinorganic Chemistry and Applications.*, **2013**, *1*. https://dx.doi.org/10.1155/2013/549549.
37. Agbo, N. J.; Ukoha, P.O., *Int. J. Chem.*, **2010**, *20*(4), 217-225.
38. Jose, L.; Seth, M.; Ziegler, T., *J. Phys. Chem.* A., **2012**, *116*(7), 1864-7.
39. Robert, M. S.; Henderson B. K.; David J. K. Spectrometric Identification of Organic Compounds. **2005**, seventh Ed., John Wiley and sons Inc., Hoboken, 101-108.
40. Konstantinovic, S.S.; Radovanovic, B. C.; Cakic, Z.; Vasic, V., *J. Serb. Chem. Soc.*, **2003**, *68*(8-9), 641-647.
41. Mehta, B. H.; Vengurlekar, V. P., *Asian J. of Chem.*, **1999**, *11*(2), 397-400.
42. Agarwal, R.K.; Singh, L.; Sharma, D. K., *Bioinorg. Chem. Appl.*, **2006**, 1-10.
43. Hegazy, W. H.; Gaafer, A. E.-D., *Am. Chem. Sci. Journal.*, **2012**, *2*(3), 86-99.